Structural Engineering and Mechanics, Vol. 6, No. 7 (1998) 801-815
DOI: http://dx.doi.org/10.12989/sem.1998.6.7.801

Analysis of unreinforced masonry (URM) walls and evaluation of retrofitting schemes for URM structures

Sanjay Mehta †

Lichtenstein Engineering Associates, 350 5th Ave, New York, NY 10118, U.S.A.

M.A. Saadeghvaziri ‡

Department of Civil and Environmental Engineering, New Jersey Institute of Technology, Newark, NJ 07102, U.S.A.

Abstract. An overview of an analytical model to predict mortar joint failure in unreinforced masonry (URM) structures is presented. The validity of the model is established by comparison with experimental results at element level as well as structure level. This model is then used to study the behavior of URM walls and two commonly used retrofitting schemes. Finally, effectiveness of the two retrofitting schemes in increasing strength and stiffness of existing URM walls is discussed.

Key words: masonry waus; seismic; mortar; joint; interface; retrofitting.

1. Introduction

Studies from previous earthquakes indicate that URM construction is one of the most hazardous forms of construction. Seismic retrofitting of such structures is very essential in order to reduce their potential for damage to life and property in case of a seismic event. Retrofitting often requires adding a new structural system. The response of original and new structural system as well as their interaction needs to be considered for effective performance of the retrofitted structure. It is therefore important to correctly understand and predict the response of existing URM structures in linear as well as nonlinear range before implementing any strengthening scheme. Although guidelines may be available for specific strengthening schemes, their relative merits will depend on the specific case under consideration. In such a case an analytical model can be a great tool in comparing the effectiveness of various retrofitting options.

Substantial portion of the existing masonry construction was built using weak sand-lime mortar joints and strong brick units. The ultimate strength of such URM structures under combination of lateral and vertical loads is mainly dictated by failure of the mortar joints

† Project Engineer
‡ Associate Professor

which can be defined in terms of stresses in the joints (Ali and Page 1986). Thus, an analytical model should be able to predict mortar joint failure and consequent redistribution of stresses. The model should also be practical for day-to-day use.

In this paper an overview of such a model which includes a mechanism to predict mortar joint failure is presented. This model can be used for retrofitting projects involving existing URM construction built with weak mortar and strong bricks. The model has been incorporated in the general purpose finite element software, ANSYS (Rev 4.14) for day-to-day use. Using this model and other options available in the program ANSYS, two retrofitting schemes for URM structures are studied. The effectiveness of these schemes in increasing strength and stiffness of URM walls is also discussed.

2. Overview of analytical model for mortar joints

2.1. Element formulation

Ngo and Scordelis (1967) used uncoupled springs to model bond failure in reinforced concrete beams. A similar concept can be used for modeling joints in URM structures if stiffness of the springs can be derived from material and geometric properties of mortar joints. Fig. 1 shows a typical joint element and its idealization using the spring model. Analytical evaluation will give normal stiffness ***Kn*** equal to **1/2(Exh/b)** and shear stiffness ***Ks*** equal to **1/2(Gxh/b)**, where ***E*** is the modulus of elasticity, ***G*** is the shear modulus, ***h*** is the length of the joint element, and ***b*** is the thickness of the joint element. Alternatively, the stiffness of the springs can be determined experimentally as described by Goodman *et al.* (1986), Page (1978). This concept is equivalent to diagonal matrix of elastic interface parameters used by Lotfi and Shing (1994). Stresses in the joints will be the average of forces in the springs at two ends of the joint element divided by its length. Once stresses in the joint element are available, the joint failure can be modeled using the failure surface described next.

2.2. Joint failure surface

Corresponding to the element formulation discussed in the previous section, the failure

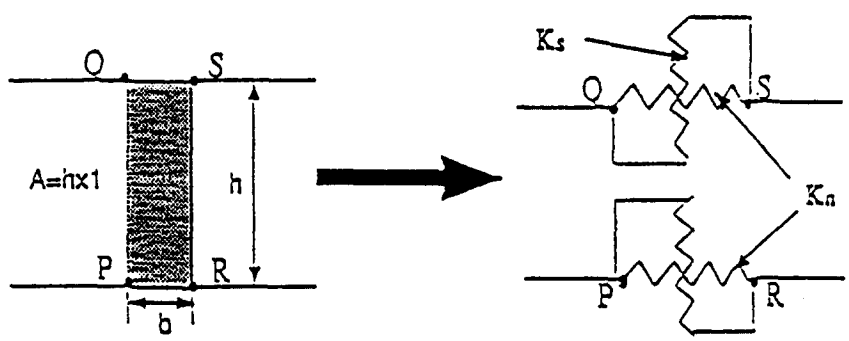

Fig. 1 Joint element and its idealization

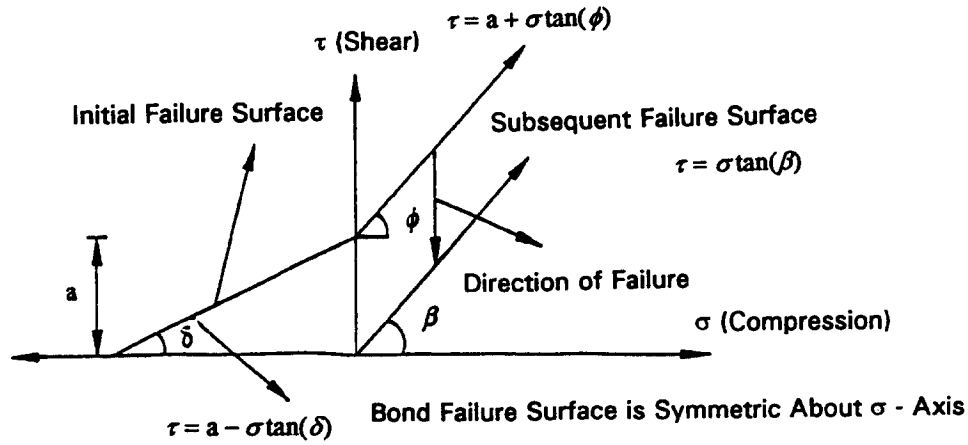

Fig. 2 Joint failure surface

surface used to check the joint failure should be determined by normal stress and shear stress in the joint. Fig. 2 shows the joint failure surface used in the present study. This failure surface is similar to the one used by Page, who performed tests on URM blocks to develop the failure surface (Page 1978). In the compression-shear zone the first failure of the joints will be governed by the "initial failure curve" (IFC) which is same as that used by Page. Initial failure curve permits the modeling of the initial bond strength of the joints. Once the joint element fails, the initial strength will not be available for resisting additional shear stresses developed in the joint. Thereafter, the failure will be governed by the "subsequent failure curve" (SFC) which is based on Coulomb's friction law. In the tension-shear zone, shear resistance decreases with an increase in tension and the failure envelope in this region is similar to that suggested by Page. No shear resistance is available in this zone after initial failure of the joint. Hence, the SFC in the tension-shear zone reduces to a point at the origin. A simple numerical technique of joint opening and closing, as discussed later, is used to avoid problems associated with a sharp corner in the IFC. The proposed failure surface with this technique provides a simple and effective method of joint modelling and can be used in lieu of a three parameter hyperbolic yield criterion (Hamid and Benson 1994), for most of the practical problems. The consequence of joint failure of a typical joint element is discussed next.

If the joint element fails in the tension-shear zone, both normal and shear stresses in the joint element are released. Both normal and shear stiffness become zero (1.0E-6) in this case.

In case of joint element failure in the compression-shear zone, only shear stress in excess of the frictional capacity is released, and the shear stiffness is reduced to zero (1.0E-6). Normal stress is transmitted across the joint and normal stiffness remains unchanged (elastic).

To achieve convergence in the case of rapidly changing contact conditions (from tension-shear to compression-shear), gap closing can be achieved in two stages (Bathe and Chaudhary 1985). Assume that the converged solution with proper knowledge of stresses in all the joint elements is available. Incremental load/displacement is then applied.

Status of all the joint elements is checked. If the open interface has closed (a decision based on the normal stress), elastic stiffness is assigned to the element but no forces are transmitted across the joint. In the subsequent iterations forces will be transferred across the joint if the joint element remains closed. Both normal stiffness and shear stiffness become

elastic if unloading is detected in the joint element.

This model was implemented in ANSYS using user programmed routines for element formulation and plasticity.

3. Verification examples

3.1. Comparison with recent developments

Recently Sharma and Desai (1992) developed a thin layer model for predicting the joint behavior. This model was verified with experimental load deflection curves obtained from shear tests. Fig. 3a shows the mesh used by Sharma and Desai to simulate the joint behavior. Mesh shown in Fig. 3b was used in the present study. Fig. 4 compares load deflection curve obtained from the models and the experiment. Good agreement is found between

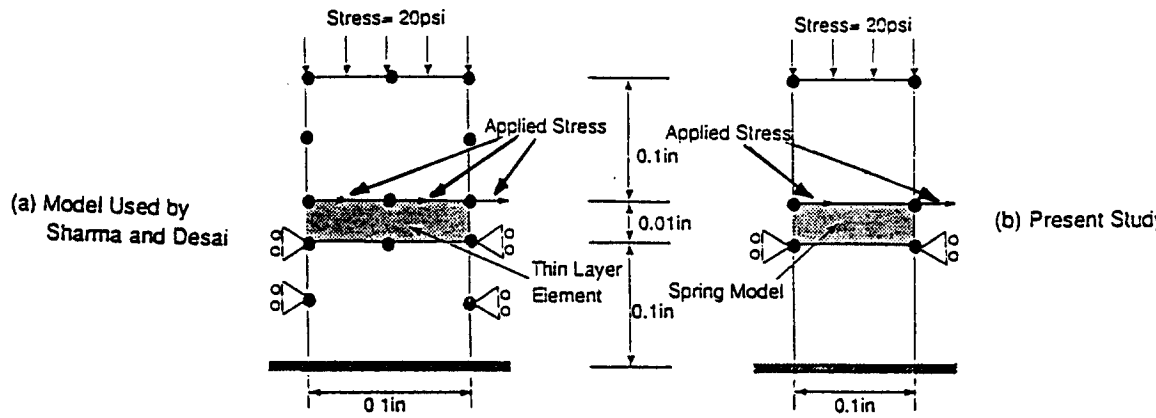

Fig. 3 Analytical models for shear test-section 3.1

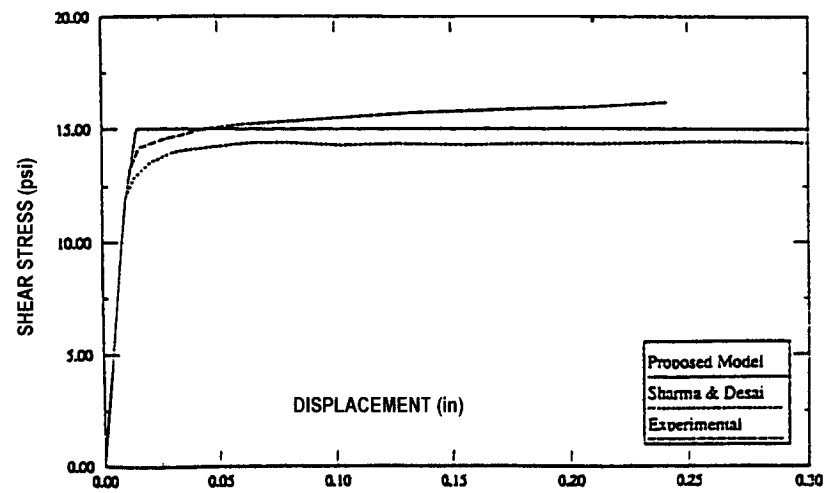

Fig. 4 Comparison of load deflection curves for shear test-section 3.1

experimental results and analytical predictions.

It should be noted that the comparison is done at the element level. The system shown in Figs. 3a and 3b do not have any redundancy as far as joint failure is concerned. Thus, the most important aspect of joint failure in a redundant system such as URM walls and consequent stress redistribution can not be verified using element level tests. To demonstrate this aspect of the present model, the ultimate strength and load-deflection response of a URM wall is compared with the experimental results.

3.2. Nonlinear analysis of URM wall

Nonlinear analysis of the wall shown in Fig. 5 was performed. This wall was tested by Woodward and Rankin (1984). Plane stress elements were used to model the concrete bricks.

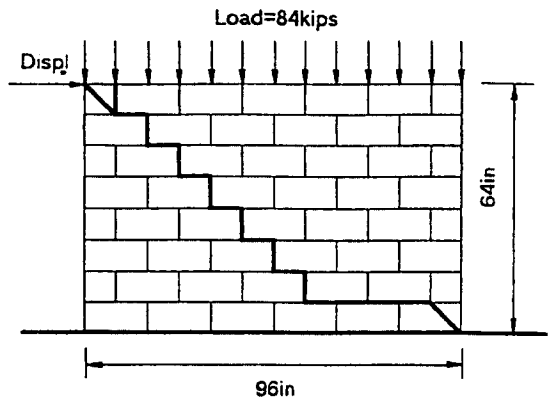

Fig. 5 Experimental cracking pattern of URM wall (Woatward and Rankin 1984)

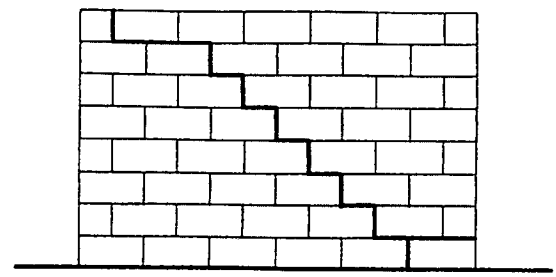

Fig. 6 Predicted cracking pattern

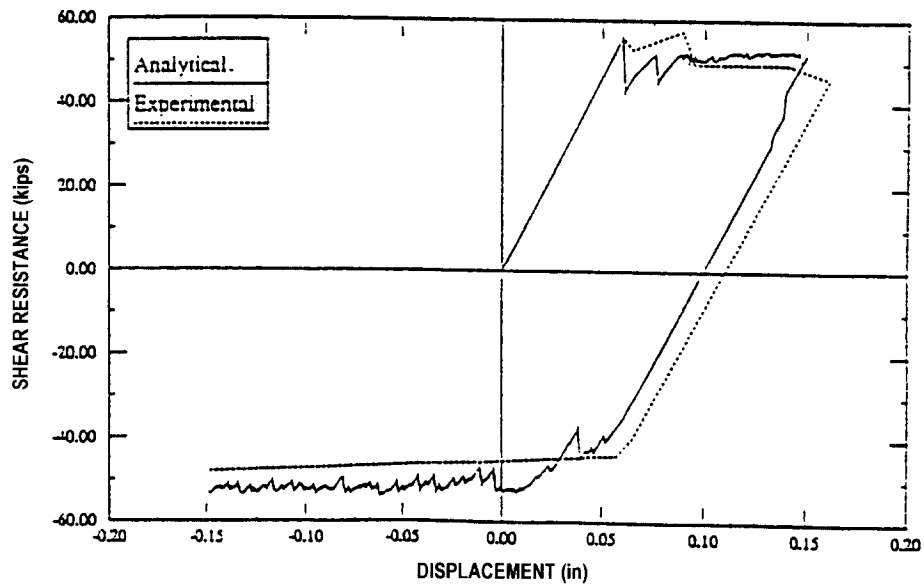

Fig. 7 Comparison of load deflection curves for URM wall

Linear material model is used for bricks, a decision based on the experimental results which show a high level of cracking caused by joint failure and insignificant material non linearity in bricks (Fig. 5). Mortar joints were modelled using the spring model with the provision for joint failure as discussed in section 2.

Incremental lateral displacement was applied at the top edge of the wall under a constant vertical load of 84 kips. The cracking pattern predicted from the analytical model is shown in Fig. 6. Fig. 7 shows a comparison of the load deflection curves. The first crack developed in the staggered joints at the center of the wall when the lateral displacement at the top edge was 0.06 in. This crack extended further in a stair shaped fashion. Towards the corners of the wall the crack extended horizontally. It appears that the completed diagonal/horizontal crack served as a slip line along which the upper right segment of the wall translated relative to the lower left segment. Similar behavior was observed in the experiment. From the load deflection curve it can be seen that the shear strength drops immediately after the initiation of cracking, initial failure, and then increases again. Such a behavior can be explained as follows.

In the nonlinear analysis described above, stresses are released and redistributed following the failure of joint elements. This release and redistribution of stresses is decided by the direction of failure as indicated in Fig. 2. At a certain value of lateral displacement some joint elements in compression-shear zone will hit the initial failure curve. As a result, for these elements the shear strength drops from the "initial failure curve" to the "subsequent failure curve". Consequently, shear strength of the URM wall would drop for the prescribed displacement. Now the residual shear strength of elements that have failed in compression and shear will be proportional to normal force. These elements will be on the SFC. All other joint elements with normal compressive force will be within the IFC. Stresses in these remaining joint elements will increase with the increase in displacement. Consequently, shear resistance still increases after initial failure. The second drop occurs when another transition from IFC to SFC occurs for additional elements. The process continues until the crack has fully developed. Similar behavior can also be seen in the experimental load-deflection curve shown in Fig. 7.

4. Analytical evaluation of retrofitting schemes for URM walls

The analytical model described in section 2, together with various other options available in the program ANSYS, is used to study the behavior of URM walls and the performance of the retrofitting schemes. As a first step, the response of URM walls without any strengthening is evaluated. The effectiveness of the retrofitting scheme is then evaluated by comparing the increase in strength and stiffness of the retrofitted structure with the original URM walls. Three URM walls are analyzed. Same joint failure parameters are used for each wall. These parameters are consistent with the experimental results discussed in section 3.2. Thus, with reference to the joint failure surface shown in Fig. 2, a=580 lb/in, $\tan(\phi)=\tan(\beta)$=0.65, $\tan(\delta)$ =0.5, **Emortar**=1210 ksi, **Ebrick**=2420 ksi. The following nomenclature is used in the discussion of results. The first two numbers represent size of the wall in inches. This is followed by either "*W*" for a wall without an opening or "*O*" for wall with an opening. The last number represents total vertical compressive force (kips) applied to the wall. Thus, 96× 64W84 wall (discussed in section 3.2) represents a wall whose length is 96in, height is 64in and the vertical compressive load is 84 kips.

Table 1 Initial stiffness and shear strength of URM walls

Wann Name	Compression (Kips)	Initial stiffness (Kips/in)	Actual shear strength (Kips)	ACI Shear strength (Kips)	Ratio Col 4/Col 5
96×64W84	84.00	982.00	58.00	24.24	2.39
96×96W96	96.00	523.00	50.00	24.24	2.06
96×96O96	96.00	238.00	29.00	16.29	1.78

4.1. Analysis of URM walls

96×64W84 Wall: The behavior of this wall has been discussed in section 3.2.

96×96W96 Wall: The behavior of this wall was similar to that of 96×64W84 wall. The first two cracks developed in two staggered joints at the center when the lateral displacement was 0.095in. These cracks propagated towards the corners of the wall. Unlike 96×64W84 wall, no sliding was observed at the corners of the wall. Maximum shear resistance was 50 kips.

96×96O96 Wall: This wall had an opening of 32"×32" at the center. The cracking started at the top left and bottom right corners of the opening when the lateral displacement was 0.095in. The crack continued towards the corners of the wall in stair shaped fashion. Maximum shear resistance was 29 kips.

Discussion of results: Table 1 shows initial stiffness of the walls. Considering the four equations given in section 6.5.2 of ACI code (now known as Masonry Standards Joint Committee Code) for URM design (ACI 530-88/ASCE 5-88), the shear strength of all the walls will be governed by the first equation:

$$f_v = 1.5\sqrt{f_m^1}$$

Where f'm (1800 psi) is the compressive strength of the masonry. Thus, for all the walls discussed earlier, the allowable shear stress will remain the same irrespective of wall's aspect ratio, vertical compressive stress, bond strength, etc. Column 5 in Table 1 shows shear resistance of walls using this formula and column 6 gives the ratio of the maximum shear resistance obtained from the analysis to the allowable shear stress given by the ACI code. It can be seen that this ratio varies from 2.39 for the 96×64W84 wall to 1.78 for the 96×96O 96 wall.

4.2. Evaluation of retrofitting schemes

Two commonly used retrofitting schemes are analyzed. In the first scheme, hereafter, referred to as Rehab1 (extension .R1 for Tables and Graphs), a steel frame around the wall is used to strengthen the wall. As pointed out in reference (Repair and Retrofit of Existing Structures), this is a frequently used method to provide strength and ductility to existing URM structures. In the second scheme, denoted by Rehab2 (extension .R2 for Tables and Graphs), steel bracing along the diagonals of the walls is used to strengthen the wall.

4.2.1. Design of Rehab1

For design of the frame surrounding a wall (Fig. 8), the concept of relative stiffness was

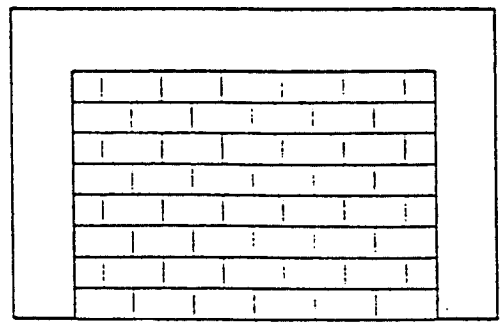

Fig. 8 Rehab1, Frame surrounding the wall

used. Relative stiffness parameter, introduced by Stafford-Smith (1962) for the design of infilled frames, is the ratio of wall stiffness to frame stiffness. Values ranging from 4 to 12 have been reported in the literature (Page, Kleeman and Dhanasekar 1985). The initial stiffness of the URM walls was determined from the load deflection curves and is given in Table 1. A relative stiffness parameter between 3 to 4 was selected to determine the moment of inertia of the columns in the steel frame. Four noded isoparametric plane stress elements, with extra shape functions to improve the flexural behavior (Taylor, Beresford and Wilson 1976), were used to model the steel frame.

Two possibilities were considered. In the first case, the compression in the Rehab walls was kept the same as that in the original URM walls (Table 1). This total compression would be distributed between the frame and the wall according to their axial stiffnesses. In the second case, the total compressive force on the retrofitted wall was increased so that the portion going to the masonry wall would be the same as the vertical force on the original URM walls (Table 1).

For linear analysis, two cases for interface conditions were considered. The first case assumed no bond between the frame and the wall. In the second case full interaction between the frame and the wall was assumed. For nonlinear analysis, only the second case (i.e., perfect interaction between wall and frame) was assumed. A bilinear kinematic hardening (von Mises) rule was used to model yielding of the steel frame. This hardening rule has been experimentally verified for ductile metals like steel (Chen and Han 1987). The joint failure

Table 2 Comparison of initial shear stiffness of wall and frame

		No interaction between frame and wall			Perfect bond between frame and wall		
Wall Name	Column depth (in)	K_w^1 kips/in	K_f^2 kips/in	K_w/K_f	K_w^1 kips/in	K_f^2 kips/in	K_w/K_f
96×64W.R1	12.20	982.00	284.50	3.45	992.00	708.00	1.40
96×96W.R1	15.00	523.00	135.60	3.86	610.00	505.00	1.21
96×96O.R1[3]	12.00	238.00	73.00	3.26	454.00	235.00	1.93
96×96O.R1	15.00	238.00	135.60	1.76	438.00	305.00	1.44

[1] K_w is shear stiffness of wall,
[2] K_f is shear stiffness of frame and
[3] Linear analysis only.

surface, as discussed before, was used to model joint failure. Brick elements were assumed to be linear.

Discussion of results: Table 2 shows shear stiffness of the frame and the wall for two possibilities, no frame-wall interaction and full frame-wall interaction. No interaction between the frame and the wall implies that each one is free to deform so as to have the minimum strain energy in each component. The relative stiffness based on no interaction was used to design the frame as discussed in the earlier section. If perfect bonding is assumed between the frame and the wall, stiffness of both the wall and the frame increases. It can be seen that the increase in stiffness of the frame is significantly more than the increase in stiffness of the wall (149% for frame and negligible for wall, in the case of 96×64W.R1). Consequently, the wall's relative stiffness decreases and the contribution of the frame to resisting the lateral force increases significantly.

In the first case of nonlinear analysis, assuming full interaction, total compression on the frame-wall system was the same as compressive force on the corresponding URM wall discussed in section 4.1 and given in Table 1. Two solid (without opening) walls were

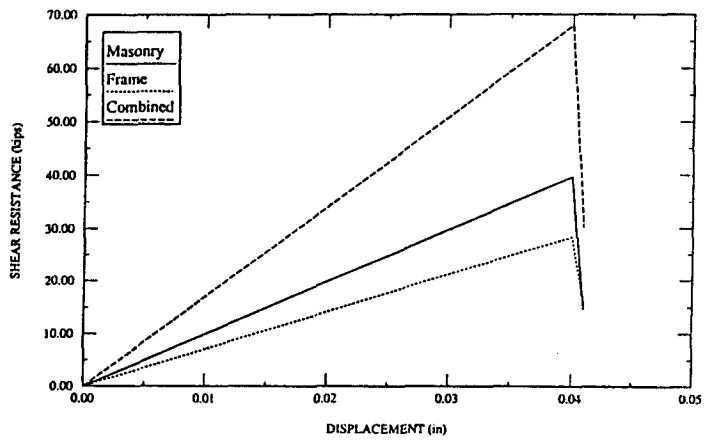

Fig. 9 Load deflection curves-96×64W.R1, Case 1

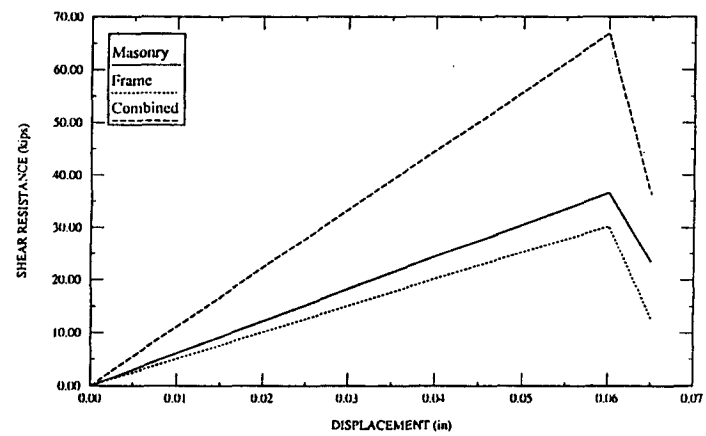

Fig. 10 Load deflection curves-96×96W.R1, Case 1

Table 3 Comparison of Rehab1, Case 1: Total compression same as Table 1-Col 2

Wall Name	Ratio of axial stiff frame wall	Wall shear strength (kips)	Frame shear strength (kips)	Total shear strength (kips)	Increase in strength w.r.t original wall
96×64W.R1	4.71	40.00	29.00	69.00	20%
96×96W.R1	4.49	36.50	30.00	66.50	33%

analyzed for this case. Figs. 9 and 10 show load-displacement curves for 96×64W.R1 and 96×96W.R1. From Table 3, it can be seen that the axial stiffness of the frame is four to five times that of the URM wall. The total compressive force was distributed according to these stiffnesses, resulting in significant reduction in the compressive force on the wall. Therefore, the shear resistance at the beginning of cracking is significantly smaller as compared to the corresponding value for URM wall alone. From load deflection curves it can be seen that the failure of the system is sudden. Such a behavior can again be attributed to the significant reduction in the compression on the wall and can be explained as follows.

Shear resistance of the joints after the first failure is proportional to the compressive force and would be close to zero if the compressive force is very small. Consequently, a large amount of shear force will be released due to failure of the joints, causing a crack to develop fully in the single load step which results in sudden failure. In both cases, failure was governed by a horizontal crack in the bed joints just above the wall base. The reduction in the shear strength of the wall offsets the increase in capacity due to the addition of the steel frame. As a result, the increase in strength of the combined system over corresponding URM wall is 20% for 96×64W.R1 and 33% for 96×96W.R1. It can be concluded that interaction of both axial and flexural/shear stiffness needs to be considered when designing a strengthening scheme.

In the second case, total compressive force on the system was increased so that the portion going to the wall would be equal to the total vertical force on the corresponding URM wall alone as discussed in section 4.1 (Table 1). See Figs. 11 to 13 for load displacement curves. Table 4 shows the total compression and shear strength of each

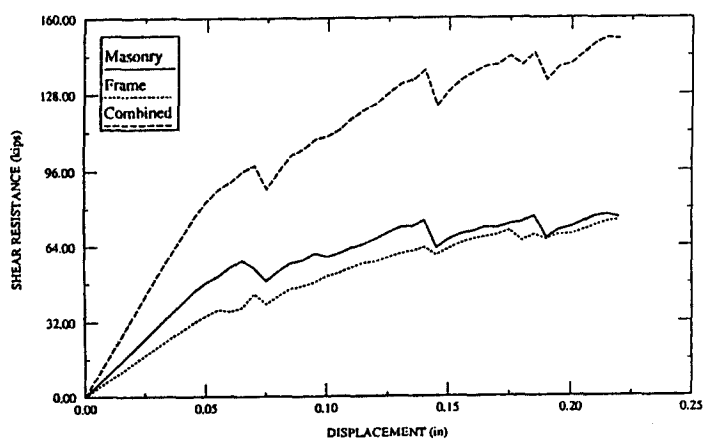

Fig. 11 Load deflection curves-96×64W.R1, Case 2

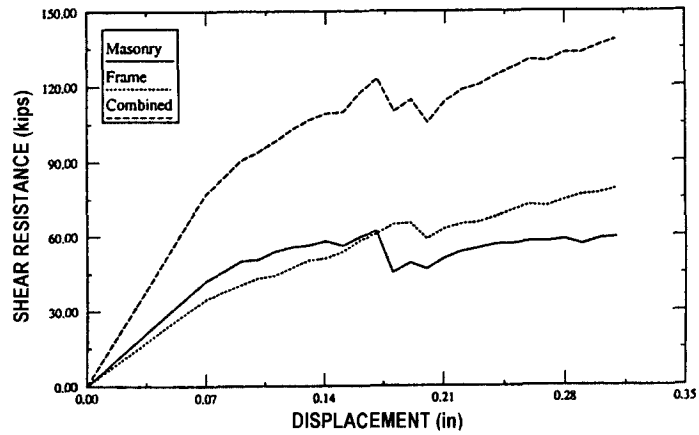

Fig. 12 Load deflection curves-96×96W.R1, Case 2

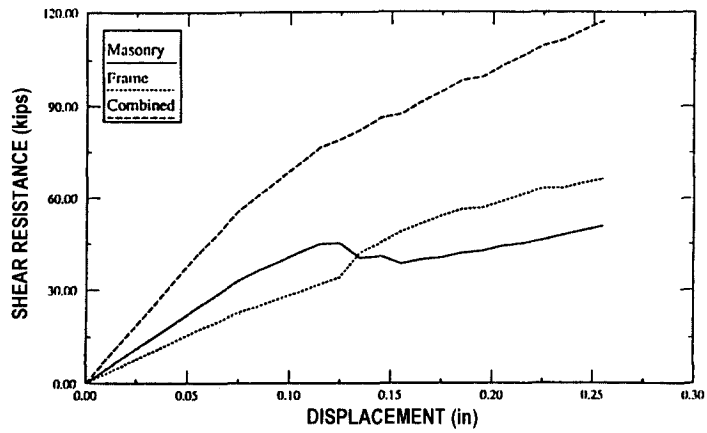

Fig. 13 Load deflection curves-96×96O.R1, Case 2

Table 4 Comparison of Rehab1, Case 2: Total compression increased

Wall Name	Total compression (kips)	Wall shear strength (kips)	Frame shear strength (kips)	Total shear strength (kips)	Increase in strength w.r.t original wall
96×64W.R1	396.00	75.00	75.00	150.00	159%
96×96W.R1	523.00	60.00	78.00	138.00	176%
96×96O.R1	738.00	51.00	66.00	117.00	303%

component in the system. From load displacement curves it can be seen that the stiffness of the frame is perturbed by the stiffness change in the wall. Wall-frame interaction is the cause for such a perturbation. With the failure of elements in the wall, its deflected shape changes. This influences the deflected shape of the frame due to perfect bond conditions at the interface, resulting in disturbance in the frame stiffness. When the failure of the combined system occurred, the steel frame had yielded.

The increase in shear capacity over the original URM wall is 159% for 96×64W.R1, 176%

for 96×96W.R1, and 303% for 96×96O.R1.

4.2.2. Design of Rehab2

As mentioned before, this scheme uses diagonal bracing for strengthening URM walls (Fig. 14). In order to compare the relative merits of the two retrofitting schemes, the total volume of steel used in both rehab schemes was almost equal. Cross sectional area of tie-down members and bracing members was kept equal. For the case of wall with opening, additional steel frame was placed around the opening. The depth of this frame was equal to the thickness of the blocks (Fig. 15).

Discussion of results: Similar to case 2 of Rehab1, total compression was increased so that the part going to the wall would be the same as the compression on the corresponding URM wall discussed in the second section of this paper (Table 1). Load deflection curves for three examples are shown in Figs. 16 to 18. The walls exhibited a shear mode of failure in all three cases. The diagonal bracing member started yielding at the point of maximum shear resistance. From the load deflection curves for solid (without opening) walls, it can be seen that cracking

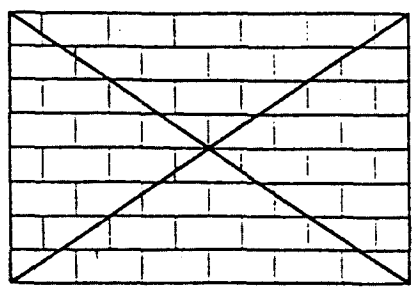

Fig. 14 Rehab2, bracing across the wall

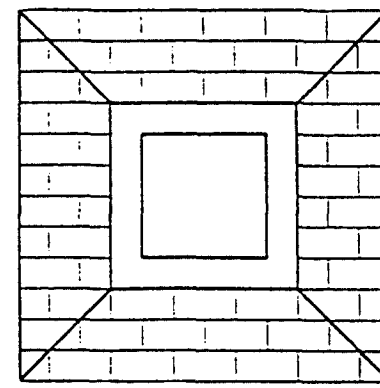

Fig. 15 Rehab2, wall with opening

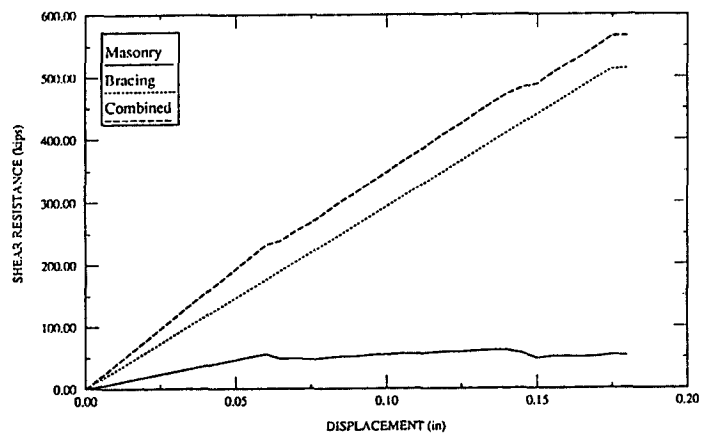

Fig. 16 Load deflection curve for 96×64W.R2

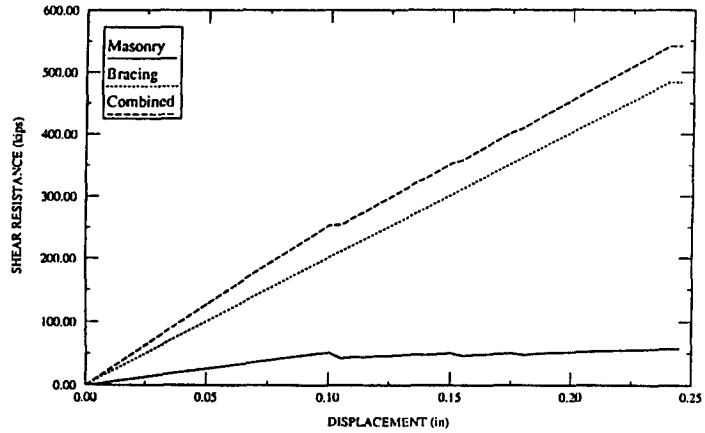

Fig. 17 Load deflection curve for 96×96W.R2

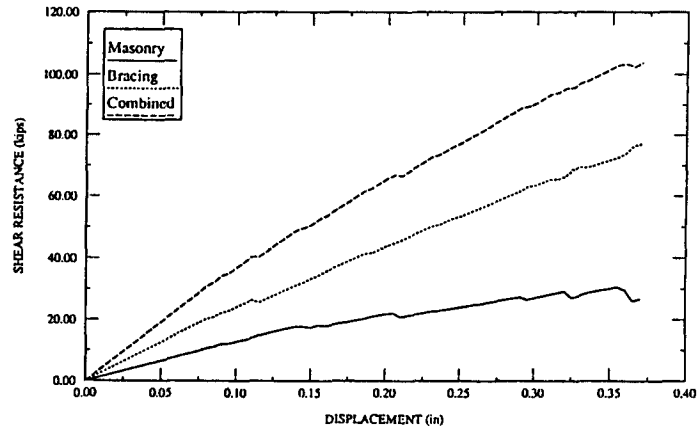

Fig. 18 Load deflection curve for 96×96O.R2

in the masonry developed when the displacement was 0.06in for wall 96×64W.R2 and 0.1in for 96×96W.R2. The shear resistance of solid walls remained almost constant thereafter. As already mentioned, after the first failure of joints in URM walls, shear resistance is proportional to friction and thus the compressive load. Thus, if enough compressive load is applied on the URM walls, the resistance of the combined system (i.e., both wall and bracing) will be the sum of the shear resistances of the individual components. One of the important points regarding the performance of the bracing system is buckling of compression members. Simple hand calculations indicated that shear strength based on the buckling of diagonal bracing members was more than the shear resistance of the bracing system given in Table 5.

5. Comparison of Rehab schemes

Table 6 shows the effectiveness of the two rehab schemes in increasing the shear capacity of URM walls. For solid walls, the increase in capacity of the combined system is significantly higher for Rehab2 as compared to Rehab1. Rehab1 increases capacity of solid URM walls by

Table 5 Comparison of Rehab2: Total compression increased

Wall Name	Total compression (kips)	Wall shear strength (kips)	Bracing shear strength (kips)	Total shear strength (kips)	Increase in strength w.r.t original wall
96×64W.R2	325.00	53.00	512.00	565.00	874%
96×96W.R2	457,00	49.00	484.00	533.00	966%
96×96O.R2	638.00	27.00	77.00	104.00	258%

Table 6 Effectiveness of Rehab Schemes in increasing strength of URM walls

Wall Name	Rehab 1 (Case 2)	Rehab 2
96×64W	159%	874%
96×96W	176%	966%
96×96O	303%	258%

a factor of 1.5 to 2, whereas Rehab2 increases the capacity of URM walls by a factor of 8 to 10. In a bracing system the axial stiffness of steel members is used to resist the lateral force. In the frame system lateral load is resisted by bending/shear stiffness of columns. For the given cross section and length, transfer of forces through axial force is more effective. Consequently, Rehab2 offers higher resistance as compared to Rehab1. The ductility requirement is inversely proportional to the strength of the system. Thus, a larger increase in strength of the retrofitted scheme by using the bracing system would require a lesser ductility demand as compared to frame-wall system. In the case of the wall with an opening, Rehab2 does not show any advantage over Rehab1. The presence of an opening does not provide a continuous path across the diagonals for the transfer of lateral force based only on axial deformation.

6. Conclusions

The joint model described in this paper predicts the failure of mortar joints in URM structures and consequent stress redistribution. Incorporation of this model in general purpose finite element software, ANSYS, permits effective analyses of URM structures and their retrofitting schemes.

Superimposed dead load is helpful in increasing the lateral resistance of URM walls. It is important not to redistribute this compressive force while retrofitting the URM walls provided there is no potential of crushing due to excessive compression. This is also advantageous from construction point of view as it may avoid jacking the load supported by the URM walls. Strong connection between URM wall and surrounding steel frame is desirable as it tends to increase the participation of steel frame in resisting lateral force.

For the same amount of steel used in the force resisting members, an increase in shear strength due to the addition of a bracing system is more effective compared to that derived from a frame system. An increase in strength is very important because of the brittle behavior of URM walls. Ductility requirement is inversely proportional to strength. Thus, the

availability of higher strength using a bracing system requires lower ductility demand.

Acknowledgements

This work was supported in part by the National Science Foundation under grant BCS-9109115 and the Department of Civil and Environmental Engineering at New Jersey Institute of Technology.

References

ACI 530-88/ASCE 5-88, "Building code requirements for masonry structures."

Ali, S. and Page, A. (1986), "A failure criterion for mortar joints in brickwork subjected to combined shear and tension", *Masonry International*, (9), December.

ANSYS, *Engineering Analysis System*, Swanson Analysis Systems Inc., Rev 4.1A, Houston, Pennsylvania 15342.

Bathe, K.J. and Chaudhary, A. (1985), "A solution method for planar and axi-symmetric contact problems", *International Journal of Numerical Methods in Engineering*, **21**, 65-88.

Chen, W.F. and Han, D.J. (1987), *Plasticity for Structural Engineers*, Springer-Verlag, ISBN 0-387-96711-7.

Goodman, R.E., Taylor, R.L., and Brekke, T.L. (1968), "A model for mechanics of jointed rock", *Proceedings, ASCE, Journal of Soil Mechanics and Foundations Division*, SM3, 637-658, May.

Hamid Lotfi and P. Benson Shing (1994), "Interface model applied to fracture of masonry structures", *Journal of Structural Engineering*, **120**(1), January.

Ngo, D. and Scordelis, A.C. (1967), "Finite element analysis of reinforced concrete beams", *ACI Journal*, 152-162, March.

Page, A., Kleeman, P., and Dhanasekar, M. (1985), "An inplane finite element model for brick masonry", *New Analysis Techniques for Structural Masonry*, Chicago, Illinois, September.

Page, A.W. (1978), "Finite element model for masonry", *ASCE, Journal of Struct. Division*, **104**(ST8), August.

Phil M. Ferguson, "Repair and retrofit of existing structures", Structural Engineering Laboratory, The University of Texas at Austin, *PMFSEL Report* 87-6, 44-49.

Sharma, K.G. and Desai, C.S. (1992), "Analysis and implementation of thin-layer element for interfaces and joints", *Journal of Engineering Mechanics*, **118**(12), 2442-2463, December.

Stafford-Smith, B. (1962), "Lateral stiffness of infilled frames", *Journal of Structural Division, ASCE*, **88**(ST6), 183-189.

Taylor, R.L., Beresford, P.J., and Wilson, E.L. (1976), "A non-conforming element for stress analysis", *International Journal for Numerical Methods in Engineering*, 10, 1211-20.

Woodward, K. and Rankin, F. (1984), "Influence of vertical compressive stress on shear resistance of concrete block masonry walls", *NSBIR* 84-2929, U.S. Department of Commerce, October.